

Differential-Geometric Modelling and Dynamic Simulation of Multibody Systems

Andreas MÜLLER¹⁾ and Zdravko TERZE²⁾

1) University Duisburg-Essen

Chair of Mechanics and Robotics
Lotharstrae 1, **Germany**

2) Fakultet strojarstva i brodogradnje Sveučilišta
u Zagrebu (Faculty of Mechanical Eng. &
Naval Arch, University of Zagreb),
Ivana Lučića 5, HR-10000 Zagreb
Republic of Croatia

zdravko.terze@fsb.hr

Keywords

CAD

Constraint violation

Lagrange equations

Lie groups

Multibody systems

Numerical integration

Woronetz equations

Ključne riječi

CAD

*Diskretni mehanički sustavi s kinematičkim
vezama*

Jednadžbe Woronetz

Lagrangeove jednadžbe

Lieve grupe

Numerička integracija

Numeričke povrede kinematičkih ograničenja

Received (primljeno): 2009-04-30

Accepted (prihvaćeno): 2009-10-30

1. Introduction

Geometric methods in dynamics and control have become widely established and valued approaches. The actual meaning of 'geometric' varies with the context in which it is used. It generally refers to the differential geometry of the mathematical structures underlying a dynamic system. As an example, non-linear control theory for continuous systems is solely built upon the differential-geometry of the control system [5, 21-23]. In other words, generally, one deals with control systems on manifolds. Another area that makes use of geometric

Original scientific paper

A formulation for the kinematics of multibody systems is presented, which uses Lie group concepts. With line coordinates the kinematics is parameterized in terms of the screw coordinates of the joints. Thereupon, the Lagrangian motion equations are derived, and explicit expressions are given for the objects therein. It is shown how the kinematics and thus the motion equations can be expressed without the introduction of body-fixed reference frames. This admits the processing of CAD data, which refers to a single (world) frame. For constrained multibody systems, the Lagrangian motion equations are projected to the constraint manifold, which yields the equations of Woronetz. The mathematical models for numerical integration routines of MBS are surveyed and constraint gradient projective method for stabilization of constraint violation is presented.

Diferencijalno-geometrijsko modeliranje i dinamička simulacija diskretnih mehaničkih sustava s kinematičkim vezama

Izvornoznanstveni članak

U radu je prikazano matematičko modeliranje kinematike diskretnih mehaničkih sustava s kinematičkim vezama pomoću Lievih grupa. Kinematika sustava parametarizirana je koristeći vijčane koordinate zglobova kinematičkog lanca. Nastavljajući se na takav kinematički model, Lagrangeove dinamičke jednadžbe gibanja sustava izvedene su u nastavku rada. Koristeći takav pristup, pokazano je kako se kinematički model, a također i dinamičke jednadžbe gibanja mehaničkog sustava, mogu izvesti bez upotrebe lokalnih koordinatnih sustava vezanih za pojedina tijela kinematičkog lanca. Takvo matematičko modeliranje omogućava izvornu upotrebu CAD podataka koji se, u pravilu, izražavaju u jedinstvenom koordinatnom sustavu. U slučaju dodatnih kinematičkih ograničenja narinutih na sustav, jednadžbe gibanja izvedene su projiciranjem Lagrangeovih jednadžbi na višestrukost ograničenja, čime se model izražava u obliku jednadžbi Woronetz. U radu su, nadalje, prikazane formulacije matematičkih modela koji se koriste kao podloga numeričkih algoritama za vremensko integriranje jednadžbi dinamike, a također je, uz izrađeni numerički primjer, opisana i metoda stabilizacije numeričkih rješenja na višestrukosti ograničenja.

concepts, is the field of geometric integration [10]. The subject here is the integration of dynamic systems on manifolds, of which systems on Lie groups are special cases [12, 27].

In mechanism theory, one is concerned with the geometry of finite motions, and on velocity level with their differential geometry. As it turns out in the case of rigid multibody body systems (MBSs), the differential-geometric objects correspond to with the line geometry of the joints and bodies. The underlying reason is the isomorphism of the algebra of screws and the algebra of the Lie-group of rigid body motions [20, 34]. The latter is the

group of isometric orientation preserving transformations of the three-dimensional Euclidean space. In essence, the parameterization of screws with line coordinates gives rise to geometric treatment of differential-geometric entities. Screw theoretic considerations also gave rise to the development of advanced methods for the design of mechanisms [14, 25, 36]. Besides these geometric and kinematic applications, explicit use of the Lie group structure admits to expressed motion equations of mechanisms in a very compact and elegant way [4, 11, 17, 24, 26, 28] and also admits application of integration schemes on Lie groups [25]. The difference of classical matrix formulations and recursive formulations [1, 7-8, 32-33] is that these formulations are entirely formulated in terms of screw quantities, corresponding to the mechanism's joint geometry (by virtue of the parameterization with line coordinates). Furthermore, the coordinate invariance allows for a formulation without body-fixed reference frames and hence for the incorporation of CAD data. This fact will be emphasized throughout the paper.

The paper is organized as follows. Section 2 deals with the geometry and summarizes the representation of configurations of rigid MBSs. After recalling the graph representation of the MBS topology, configurations are expressed as elements of the 3-dimensional special Euclidean group. The configuration space is then parameterized using canonical (axis/angle) and non-canonical parameters. A formulation is given that does not need the definition of body-fixed frames. The kinematics is addressed in section 3. The closed form expression for rigid body velocities in terms of the instantaneous joint screws and the time derivatives of the parameters is given. This is a recursive relation that can also be expressed in matrix form. In section 4 the dynamics is addressed and the Lagrangian motion equations are given. Their differential-geometric meaning is briefly outlined, making use of the Riemannian metric defined by the generalized mass matrix. The motion equations are also given in matrix form. For completeness, the equations of Woronetz are given, i.e. a formulation of the motion equations of constrained MBSs, which does not involve Lagrange multipliers. In section 5 the mathematical models for numerical integration routines of MBS are surveyed. Furthermore, constraint gradient projective method for stabilization of constraint violation is addressed and a numerical example is presented.

2. MBS geometry

2.1. The topological graph of an MBS

The MBS topology is represented as an oriented graph $\Gamma = (B, J)$, where the set of vertices B represents the bodies, and the set of edges J represents the joints of the

MBS. It is assumed hereafter that Γ has one connected component. In this case Γ has $\gamma = m - N$ fundamental loops (FLs), where $m := |J|$ is the number of joints and $N := |B| - 1$. Joints and bodies are respectively denoted by J_α , $\alpha = 1, \dots, m$ and B_k , $k = 0, \dots, N$. Body B_0 stands for the ground. An edge $J_\alpha \in \Gamma$ is an unordered pair $J_\alpha \equiv (B_k, B_l)$ (for brevity, we write $\alpha \in \Gamma$ or $(k, l) \in \Gamma$ if $J_\alpha \equiv (k, l)$).

A spanning tree of Γ is denoted by $G = (B, J^G)$, and the corresponding cotree by $H(\Gamma, G) = (B, J^H)$, or simply with H . Vertex B_0 is chosen as the root of the tree. J^G is the set of tree-joints, and $J^H := J \setminus J^G$ is the set of cut-joints. G comprises N tree joints. The term cut-joint indicates that, if we 'cut' these joints, we get a tree topology.

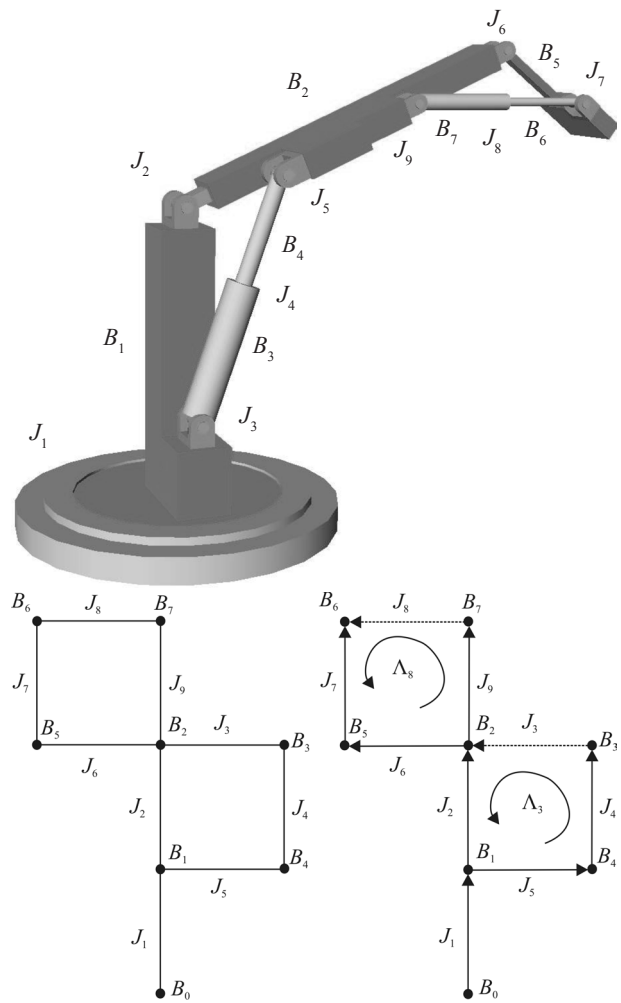


Figure 1. An example for the graph description of a MBS.

Slika 1. Primjer graf-opisa diskretnog mehaničkog sustava s kinematičkim vezama

Let G^d be the directed tree w.r.t. to the root B_0 , which is the directed subgraph of G such that to every vertex there is a path starting from the root of G (Figure 1). The directed tree induces the following ordering relation of joints and bodies:

- B_1 is the direct predecessor of body B_k , denoted by $B_1 = B_k - 1$, iff¹ $(l, k) \in G^d$ (for short $l = k - 1$)
- J_β is the direct predecessor of joint J_α , denoted by $J_\beta = J_\alpha - 1$, iff $J_\beta = (\cdot, k) \in G^d \wedge J_\alpha = (k, *) \in G^d$ (for short $\beta = \alpha - 1$)
- J_β is a predecessor of joint J_α , denoted by $J_\beta \leq J_\alpha$, iff there is a finite m , such that $\beta = \alpha - 1 - 1 \cdots - 1$ (m times -1).

Note that possibly $k - 1 = l - 1$ for $k \neq l$. E.g. in Figure 1., $J_1 = J_2 - 1, J_2 = J_6 - 1, J_6 = J_7 - 1$, so that $J_1 < J_7$. For each body B_k , there is a unique tree joint J_α connecting B_k to its predecessor, i.e. $J_\alpha = (\cdot, k) \in G^d$. This fact is denoted by $\alpha = J(k)$. In other words, body B_k is connected to B_{k-1} via J_α . Finally, $J_{\text{root}}(k)$ denotes the smallest $\alpha \leq J(k)$. In figure 1, $J(6) = 7, J(5) = 6$ and $J_{\text{root}}(k) = 1$ for all k . An orientation of G w.r.t. G^d is an indicator function s so that $s(J_\alpha) = 1$ or $s(J_\alpha) = -1$ if $J_\alpha \in G$ is respectively positively or negatively oriented w.r.t. G^d . Also $s(\alpha)$ is used for short.

Remark 1: Arithmetical operations on body or joint indices, like $l = k - 1$ and $\beta = \alpha - 1$, are to be understood according to the above index arithmetics. In particular, $k - 1$ does *not* mean that we subtract 1 from the body index k , it rather refers to the body B_{k-1} .

2.2. The configuration space of an MBS

A body-fixed is attached to each body of the MBS reference frame (RFR). We assume the existence of an inertial system, called the ground, which is referred to as B_0 . An inertial frame (IFR) is fixed at the ground, (Figure 2), and the configuration of body B_k is expressed as $C \in SE(3)_k$:

$$C = \begin{pmatrix} E & p \\ 0 & 1 \end{pmatrix}, \text{ with } E \in SO(3), p \in \mathbb{R}^3, \tag{1}$$

E is the rotation matrix and p the position vector, describing respectively the rotation and displacement of the body-fixed RFR w.r.t. to the IFR.

The configuration of the MBS is denoted by $c \equiv (C_1, \dots, C) \in SE(3)^N$. A subspace corresponds of relative transformations $G_\alpha \subseteq SE(3)$, to each joint called the motion space of J_α . This is not necessarily one of the $SE(3)$ -subgroups [34]. E.g., for revolute joints $G_\alpha \triangleq SO(2)$ is the group of rotations about a fixed axis. Denoted by R the relative configuration of the two bodies B_1 and B_k is α connected by $J_\alpha \equiv (l, k) \in \Gamma$ (Figure 2). A configuration of the MBS is admissible, only if $J_\alpha \in G_\alpha$. With these conditions, the set of admissible configurations is:

$$C_{\text{abs}} := \{c \in SE(3)^N \mid R \in G_\alpha\}. \tag{2}$$

This is called the *configuration space of a holonomic MBS in absolute representation*.

C_{abs} is a rather abstract notion that covers MBSs with arbitrary topology. If we were to use this representation for our actual computations, we would need to introduce constraints that restrict the relative motion of adjacent bodies to the motion spaces. In fact, this leads to absolute coordinate formulations. What we will do instead is to eliminate the constraints by resolving for the relative configuration of tree-joints, and introduce constraints only for the cut-joints.

2.3. The geometry of an MBS with tree-topology

2.3.1. Relative configurations

A joint $J_\alpha(l, k) \in \Gamma$, connecting bodies B_1 and B_k , is completely characterized by three consecutive transformations (Figure 2.):

- constant transformation $S_{\alpha, l}$ from the joint frame (JFR) to the RFR on B_1 ,
- constant transformation $S_{\alpha, k}$ from the JFR to the RFR on B_k ,
- variable transformation N_α of these JFRs, according to the joint's mobility, and the orientation of $J_\alpha \in \Gamma$, that determines whether N_α transforms from the JFR on B_k to that on B_1 or vice versa.

This information characterizes the joint kinematics without reference to a topological tree. By definition, $J_\alpha(l, k) \in G^d$ means that J_α connects B_k to its predecessor $B_1 = B_k - 1$. For tree-joints, the above three transformations must be combined with a transformation from B_k to B_{k-1} RFR. The function $s(\alpha)$ indicates whether $J_\alpha \in \Gamma$ is positively oriented w.r.t. to G^d . Consequently, if J_α is negatively oriented, the transformation N_α must be inverted. E.g., the meaning of a positive revolute joint angle is reversed if its orientation is opposite to the directed tree. Thus, the relative configuration from the RFR on B_k to that on B_1 is:

$$R = M_\alpha Q_\alpha, \text{ with } M_\alpha := S_{\alpha, l} S_{\alpha, k}^{-1}, Q_\alpha := S_{\alpha, k} N_\alpha^{s(\alpha)} S_{\alpha, l}^{-1}, \tag{3}$$

M_α transforms from JFR to BFR on B_1 , and Q_α from RFR on B_k to JFR on B_1 . Finally, the configuration of body B_k is given with that of its predecessor and the joint transformation R_α

$$C = C_{k-1} R_\alpha, \alpha = J(k). \tag{4}$$

Thus, the configuration of each individual body is recursively given in terms of the relative configuration of its predecessors. Therefore, we can express the MBS configuration by $r \equiv (R_1, \dots, R_N) \in C_{\text{rel}}$ where:

¹ $(k, l) \in G^d$ means that B_k is the source and B_l is the target of the edge. Notice that $(l, k) \notin G^d$, since G^d is directed.

$$C_{rel} := G_1 \times \dots \times G_N, \tag{5}$$

is called the *configuration space in relative representation*. The degree of freedom (DOF) of the MBS is the dimension of the configuration space $\delta := \dim C = \sum_{\alpha} \dim G_{\alpha}$.

Remark 2: The body-fixed RFRs are arbitrary. We can choose other RFRs, and the configurations \bar{r} in this representation are related to the original ones by $\bar{r} = grg^{-1}$, where $g \in SE(3)^N$. These configuration constitute another representation of the configuration space, say \bar{C}_{rel} . All such representations obtained by a change of body-fixed reference frames are equivalent. Moreover, the motion equations for the MBS are invariant w.r.t. such frame transformations.

2.3.2. Parameterization of the configuration space

So far we have not used any kind of joint variables, which is necessary for the actual application. This requires at least a local parameterization of the motion spaces G_{α} . There are three options: canonical coordinates of 1. or 2. kind, and non-canonical parameterization.

1) The standard choice are canonical coordinates of 2. kind. That is, Q_{α} is expressed as series of successive screw, i.e. 1-DOF, motions. E.g., a revolute joint allows for rotations about its axis of revolution, a prismatic for translations along its joint axis, a universal joint comprises successive rotations about two non-parallel axes of revolution, while a spherical joint is considered as three consecutive rotations. If J_{α} has mobility² $\nu_{\alpha} := \dim G_{\alpha}$, the individual intermediate one-parametric motions are given in terms of a set of (relative) *generalized coordinates* for J_{α} , denoted by $q^{\alpha_1}, \dots, q^{\alpha_{\nu}}$, and a set of screw coordinate vectors $Z_{\alpha_1}, \dots, Z_{\alpha_{\nu}}$ (Figure 2), such that $N_{\alpha}^{S(\alpha)}(q^{\alpha}) = e^{\alpha_1} \dots e^{\alpha_{\nu}}$. The screw coordinate vectors are expressed in the JFR either on B_l or B_k , depending on which one is the source of the oriented edge $J_{\alpha} \in G^d$. With (3),

$$Q_{\alpha}(q^{\alpha}) = e^{\alpha_1} \dots e^{\alpha_{\nu}}, \text{ where } X_i := \text{Ad}_{S_{\alpha,k}}^{-1} Z_{\alpha_i}, i=1, \dots, \nu, \tag{6}$$

and the adjointed operator matrix [20], so that the relative transformation by the tree joint is:

$$R_{\alpha}(q^{\alpha}) = Me^{\alpha_1} \dots e^{\alpha_{\nu}}, \tag{7}$$

Z_{α_i} are the coordinate vectors of the joint screws of J_{α} , w.r.t. JFR on B_k , while X_i are the crew coordinate vectors w.r.t. to the RFR on B_k .

2) Using canonical coordinates of 1. kind, $N^{S(\alpha)}(q^{\alpha}) = e^{\alpha_1} \dots e^{\alpha_{\nu}}$

$$Q_{\alpha}(q^{\alpha}) = e^{\alpha_1} \dots e^{\alpha_{\nu}}, \tag{8}$$

with X_i in (6), and R_{α} according to (3). This corresponds to the axis-and-angle parameterization of screw motions [20, 34].

3) The parameterization (6) and (8) suffer from singularities, when dealing with spacial rotations, for which a global parameterization with canonical coordinates does not exist, i.e. via the exponential map. These singularities can be avoided using Euler-parameters [20] to describe the rotation part of N_{α} . Another motivation for the use of non-canonical parameters, like Cayley-parameters, is to reduce the numerical complexity, in applications where the full range of rotation is not used.

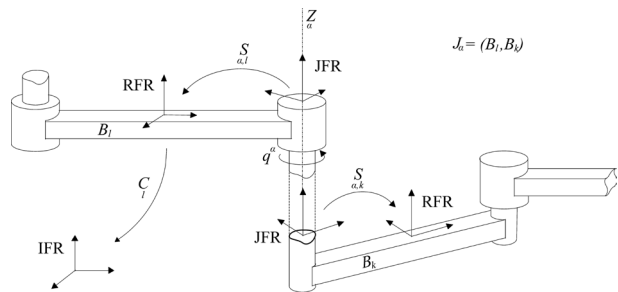


Figure 2. Relative kinematics of two bodies B_l and B_k connected by joint J_{α}

Slika 2. Relativna kinematika dvaju tijela B_l i B_k povezana kinematičkim zglobov J_{α}

In order to keep the formulation as general as possible, we will write $Q_{\alpha}(q^{\alpha})$, whenever possible, and only use the specific form, such as (6), when necessary.

The vector $(q^{\alpha}) := (q^{\alpha_1}, \dots, q^{\alpha_{\nu}}, \alpha \in G^d)$ comprises the *generalized coordinates* q^{α} of the MBS with tree-topology. The parameter manifold of an MBS with n_R revolute and n_P prismatic/screw-joints is:

$$\mathbb{V}^n = \mathbb{T}^n \times \mathbb{R}^{n_P}, n = n_R + n_P, \tag{9}$$

\mathbb{V}^n is also referred to as the *configuration space* of the MBS, and $q \equiv (q^{\alpha}) \in \mathbb{V}^n$ as its representing point.

2.3.3. Relative configurations without body-fixed joint frames

From a practitioner's point of view, the definition of body-fixed joint frames is an irksome task additional to the design process. This task is dispensable, however, as the joint kinematics can be expressed without body fixed joint frames. Such formulations are advantageous

² For compactness, we omit the joint index and write ν , if the joint is clear from the context.

when processing CAD data, which refer to a single world frame (IFR). The CAD construction serves as reference configuration to which we assign $q = 0$.

Denote with $m_k := C_k(0)$ the reference configuration of B_k , then

$$m_k = M_{\beta} \dots M_{\alpha-1} M_{\alpha}, \alpha = J(k), \beta = J_{\text{root}}(k)$$

$$Y_{\alpha_i} = Ad_{m_{\alpha_i}} X_{\alpha_i} \tag{10}$$

The Y_{α_i} are the screw coordinate vectors for joint J_{α_i} expressed in the IFR, in the reference configuration m_k . With this data, the body configurations are

$$C_k(q) = e^{\hat{Y}_{\alpha_i} q^{\alpha_i}} \dots e^{\hat{Y}_{\beta} q^{\beta}} \dots e^{\hat{Y}_{\alpha-1} q^{\alpha-1}} \dots e^{\hat{Y}_{\alpha} q^{\alpha}} m_k, \tag{11}$$

$$\alpha = J(k), \beta = J_{\text{root}}(k).$$

Remark 3: The advantage of this formulation in conjunction with CAD-data shall be stressed. CAD-systems use the IFR to express the geometry and the inertia properties of the mechanism. Consequently, in the reference configuration the RFR of all bodies coincide with the IFR, so that $m_k = I$. All that is needed are the screw coordinate vectors Y_{α_i} w.r.t. the IFR, in the reference configuration. The vector $Y_{\alpha_i} \equiv (\omega, p \times \omega + h\omega)$ is merely given in terms of the direction vector ω along the joint axis, the position vector p of some point on the axis, and the pitch h of the joint. Since the moments of inertia are also expressed in this IFR the definition of body-fixed RFRs is dispensable (section 4.).

2.4. The geometry of MBS with kinematical loops

An edge corresponds to any loop of the cotree H (which is empty for treestructures). As we have seen, the configuration of an MBS can be represented in absolute formulation (2), listing the configurations of all individual bodies plus the constraints due to the joint couplings. Alternatively, configurations can be represented in relative formulations (5), where for MBS with kinematic loops, the configuration must comply with loop closure constraints arising from cotree joints.

Hence, an MBS with kinematic loops can be modeled as an MBS with tree topology subject to holonomic constraints. That means that the cut-joints $J_{\alpha}, \alpha \in H$ are removed, and the resulting tree-system is subject to the corresponding closure conditions.

Definition 1: Denote with $v_{\alpha} = \dim G_{\alpha}$ the mobility of joint J_{α} . A smooth map $g_{\alpha} : SE(3) \rightarrow \mathbb{R}^{6-v_{\alpha}}$ is called a *local constraint map* iff $g_{\alpha}(R) = 0 \leftrightarrow R \in U \cap G_{\alpha}$, for some $U \subset SE(3)$ containing the identity. If this holds on all $SE(3)$, g_{α} is called a *global constraint map*.

Since each FL comprises exactly one cut-joint, we denote with Λ_{α} the FL containing cut-joint J_{α} . Body B_k is the *root body* of the FL iff $B_k < B_l \forall l \in \Lambda_{\alpha}$. E.g. in Figure 1. the root body of Λ_8 is B_2 and that of Λ_3 is B_1 . Denoted by H^d the directed cotree such that all $J_{\alpha} \in H$ are positively oriented. Using bodyfixed reference frames, the geometric closure condition for Λ_{α} with cut-joint $J_{\alpha} \equiv (l, k) \in H^d$ is

$$S_{\alpha,l}^{-1} C_{l,k}^{-1} C_{\alpha,k} S_{\alpha} = N_{\alpha} \tag{12}$$

The corresponding closure constraints are the independent components of (12), for which N_{α} is identically zero whenever $R \in G_{\alpha}$. These components are listed in Table 1. for some technical joints. It is indicated whether the motion space of the joint corresponds to a $SE(3)$ -subgroup. A cut-joint with mobility v_{α} yields $6 - v_{\alpha}$ (locally) independent constraint equations.

Remark 4: The distinction between local and global constraint maps should be stressed. The revolute joint is an instructive example for which the geometric constraints on the relative rotation are: $E_1^3 = E_2^3 = 0$. These plus the three position constraints, only give in fact rise to a local constraint map. This is so because the conditions on E enforce the e_3 -axes of the coupled JFRs to remain parallel, but they may have opposite directions, for which the constraints are also fulfilled.

With parameterization of the tree-joint, the cut-joint constraints yield constraints on the generalized coordinates. The overall system of $m := 6\gamma - \sum_{\alpha \in H} v_{\alpha}$ geometric constraints is summarized in:

$$g(q) = 0. \tag{13}$$

The admissible parameter space, defined by (13) is the *configuration space*:

$$V := \{q \in \mathbb{V}^n \mid g(q) = 0\}, \tag{14}$$

of the MBS with kinematic loops. V is an analytic variety comprising smooth manifolds, separated by singular points [18-19, 30-31].

3. MBS Kinematics

3.1. The kinematics of an MBS with tree-topology

The velocity of body B_k in body representation is defined as $\hat{V}_k := C_k^{-1} \dot{C}_k$. V is the twist of the RFR on B_k w.r.t. to the IFR expressed in this RFR. It is verified with (7),

$$V(q) = \sum_{\alpha \leq k} K_{\alpha}^k(q) \dot{q}^{\alpha}, \tag{15}$$

$$\text{with } K_{\alpha_i}^k := Ad_{C_k^{-1} C_m} H_{\alpha_i}, \text{ if } m \leq k, \text{ for } \alpha := J(m), \tag{16}$$

$$H_{\alpha_i} = Q_{\alpha}^{-1} \partial \alpha_i Q_{\alpha}. \tag{17}$$

Table 1. Cut joint constraints for some technical joints. E is the rotation matrix and p is the position vector describing the relative configuration (1) of the two bodies connected by the cut joint.

Tablica 1. Kinematička ograničenja za odabrane kinematičke zglobove. Rotacijskom matricom E i vektorom položaja p definirana je relativna kinematika (1) dvaju tijela koja su povezana određenim kinematičkim ograničenjem.

| DOF / SSG | Motion (Joint type) / Relativno gibanje (vrsta zgloba) | Constraints / Kinematička ograničenja | Subgroup / Subgrupa |
|-----------|---|--|---------------------|
| 1 | Translation along fixed axis (prismatic joint) / Translacija duž nepomične osi (translacijski zglob) | $E_1^2 = E_2^3 = E_1^3 = 0$ $p^1 = p^2 = 0$ | × |
| | Rotation about fixed axis (revolute joint) / Rotacija oko nepomične osi (rotacijski zglob) | $E_1^2 = E_2^3 = 0$ $p^1 = p^2 = p^3 = 0$ | × |
| 2 | Planar translation / Planarna translacija | $E_1^2 = E_2^3 = E_1^3 = 0$ $p^3 = 0$ | × |
| | Rotation + translation along same axis (cylindrical joint) / Rotacija i translacija oko iste nepomične osi (cilindričan zglob) | $E_1^3 = E_2^3 = 0$ $p^1 = p^2 = 0$ | × |
| | Two successive rotations about orthogonal axes (universal joint) / Dvije slijedne rotacije oko ortogonalnih osi (univerzalni zglob) | $E_1^2 = 0$ $p^1 = p^2 = p^3 = 0$ | - |
| 3 | Spatial translation / Prostorna translacija | $E_1^2 = E_2^3 = E_1^3 = 0$ | × |
| | Planar motion (planar joint) / Planarno gibanje (planarni zglob) | $E_1^3 = E_2^3 = 0$ $p^3 = 0$ | × |
| | Spatial rotation (spherical joint) / Prostorna rotacija (sferni zglob) | $p^1 = p^2 = p^3 = 0$ | × |
| 4 | Planar motion + spatial translation (joint macro) / Planarno gibanje + prostorna translacija (složeni zglob) | $E_1^3 = E_2^3 = 0$ | × |
| 6 | Spatial motion / Prostorno gibanje | - | × |

K is called the *Kinematic Basic Functions* (KBF) of B_k . From its definition (16) there follows immediately the recursion

$$K_k^\alpha = \begin{cases} H_{\alpha_i}, \alpha = J(k) \\ \text{Ad}_{\alpha_i}^{-1} K_{\alpha_i}, \alpha < J(k). \end{cases} \quad (18)$$

The expression for H_{α_i} depends on the choice of local coordinates on G_α (2.3.2.).

1.) For canonical coordinates of 2 kind (6):

$$H_{\alpha_i} = \text{Ad}_{\alpha_i}^{-1} X_{\alpha_i}, \text{ with } A(q^\alpha) = e^{\hat{X}_{\alpha_i}^{q^{\alpha_i}}} \dots e^{\hat{X}_{\alpha_i}^{q^{\alpha_n}}}. \quad (19)$$

2.) For canonical coordinates of 1 kind (8), using the left and right dex-p-map on se (3),

$$H_{\alpha_i} = \text{Ad}_{\alpha_i}^{-1} \begin{cases} N_\alpha^{-1} \partial_{\alpha_i} N_\alpha = \text{dexp}_{Y_\alpha}^L X_{\alpha_i}, \text{ if } s(\alpha) = 1 \\ \partial_{\alpha_i} N_\alpha^{-1} = -\text{dexp}_{Y_\alpha}^R X_{\alpha_i}, \text{ if } s(\alpha) = -1 \end{cases} \quad (20)$$

with $Y = X_{\alpha_i}^{q^{\alpha_i+1}} \dots + X_{\alpha_i}^{q^{\alpha_n}}$.

3.) Using non-canonical coordinates, H_{α_i} is of a specific form. e.g., when parameterizing the rotation matrix E in (7) with Cayley- or Euler-parameters.

For the standard choice of canonical coordinates of 2. kind, using A in (19), $K_{\alpha_i} = \text{Ad}_{\alpha_i}^{-1} \text{Ad}_{\alpha_i}^{-1} X_{\alpha_i}$ are the instantaneous joint screws of J_α expressed in the RFR of B_k . This is why K is occasionally called the *geometric Jacobian*.

With the MBS configurations $c \in C_{\text{abs}}$, we define the velocity of an MBS as $\hat{V} := c^{-1} \dot{c} \equiv (\hat{V}_1, \dots, \hat{V}_n) \in T_1 C_{\text{abs}}$. What is more important for the following is the state space $T\mathbb{V}^n$, and the generalized velocities $\dot{q} \in T_q \mathbb{V}^n$, that are related to V via (15).

3.2. Kinematics without body-fixed joint frames

The KBF can also be expressed in terms of the Y_{α_i} in (10) as:

$$K_k^{\alpha_i} = \text{Ad}_{\alpha_i}^{-1} \text{Ad}_{\alpha_i}^{-1} Y_{\alpha_i}, \alpha \leq J(k), \quad (21)$$

with $A = e^{\hat{Y}_{\alpha_i}^{q^{\alpha_i}}} \dots e^{\hat{Y}_{\alpha_i}^{q^{\alpha_n}}} \dots e^{\hat{Y}_{\alpha_i}^{q^{\alpha_i}}} \dots e^{\hat{Y}_{\alpha_i}^{q^{\alpha_n}}}, \beta = J(k)$.

This is again an expression, without reference to body-fixed JFRs.

3.3. Matrix formulation for tree-topology MBS

The recursion (18), allows for a matrix expression of V in terms of the generalized velocities. Consider a terminal body B_k of the topological tree, and the (unique)

path from B_k to B_0 . Let us, for the moment, assume that the bodies and joints of this path are numbered increasingly with $1, 2, \dots, k$. Combining the corresponding KBFs to

$$K_k := \begin{pmatrix} K_1 \\ \vdots \\ K_k \end{pmatrix}, \tag{22}$$

then $K_k = A_k H_k$, with $H_k := \text{diag}(H_1, \dots, H_k)$ and

$$A_k := \begin{pmatrix} I & 0 & \dots & 0 \\ \text{Ad}_{C_2^{-1}C_1} & I & & \vdots \\ \vdots & & \ddots & \\ \text{Ad}_{C_{k-1}^{-1}C_1} & & & I & 0 \\ \text{Ad}_{C_k^{-1}C_1} & \text{Ad}_{C_k^{-1}C_2} & \dots & \text{Ad}_{C_k^{-1}C_{k-1}} & I \end{pmatrix}. \tag{23}$$

The $H_\alpha \equiv (H_{\alpha_1}, \dots, H_{\alpha_{v_\alpha}})$ are $6 \times v_\alpha$ matrices according to the mobility of J_α , and I and 0 is respectively the 6×6 identity and zero matrix. With our primary choice of coordinates, the $H_{\alpha_i} \equiv X_{\alpha_i}$ are constant.

The items of A_k and H_k are obvious, in terms of arbitrary body indices. In summary, combining in K the K_k matrices of all terminal bodies, the MBS velocity is:

$$V = K \dot{q} \tag{24}$$

The structure of K reflects the tree-topology of the MBS. It is interesting to notice that the lower block triangular matrix can be expressed as $A_k = (I - D_k)^{-1} = I + D_k + D_k^2 + \dots + D_k^N$, with help of the nil-potent matrix

$$D_k = \begin{pmatrix} 0 & \dots & 0 \\ \text{Ad}_{C_2^{-1}C_1} & & \vdots \\ 0 & \ddots & \\ \vdots & & \\ 0 & \dots & 0 & \text{Ad}_{C_k^{-1}C_{k-1}} & 0 \end{pmatrix}, \tag{25}$$

that only comprises the relative configurations $C^{-1}C$. This is a matrix version of the recursion (18).

3.4. Partial derivatives of the KBFs

Due to the recursive formulation in terms of relative configurations, it holds:

$$\begin{aligned} \partial_{q^\beta} K_{\alpha_i} &= \text{Ad}_{C_m^{-1}C_m} \partial_{q^\beta} H_{\alpha_i}, \text{ if } \alpha = \beta \\ &+ [K_{\alpha_i}, K_{\beta_j}], \text{ if } \alpha < \beta, \text{ for } \beta \leq J(k), \alpha = J(m). \end{aligned} \tag{26}$$

For our standard choice of canonical coordinates of 2nd kind, (26) simplifies to

$$\partial_{q^\beta} K_{\alpha_i} = [K_{\alpha_i}, K_{\beta_j}], \alpha \leq \beta \leq J(k), i < j. \tag{27}$$

Computationally, (27) is very easy to evaluate, since in vector representation the Lie bracket of two $\hat{X}_1, \hat{X}_2 \in se(3)$ is $[\hat{X}_1, \hat{X}_2] = (\omega_1 \times \omega_2, \omega_1 \times v_2 + v_1 \times \omega_2)$. We thus arrive at a very compact expression for the body acceleration of B_k

$$\dot{V} = K_b \ddot{q}^b + [K_b, K_c]^b \dot{q}^c, b \leq c \leq \alpha_v, \alpha = J(k). \tag{28}$$

We use the summation convention over repeated indices: $A_{ab}x^b \equiv \sum_b A_{ab}x^b$. As the individual KBFs can be combined to K , so can their derivatives, to give the differential $dK(q, x) := \partial_a K(q)x^a$. Using $[K_{\alpha_i}, K_{\beta_j}] = \text{Ad}_{C_k^{-1}C_m} [K_m^{\alpha_i}, H_{\beta_j}] = -\text{Ad}_{C_{-1}C_m} \text{ad}_{H_{\beta_j}} K_m^{\alpha_i}$, $\beta = J(m)$, and the matrix

$$\text{ad}_x = \begin{pmatrix} \hat{\omega}_X & 0 \\ \hat{p}_X & \hat{\omega}_X \end{pmatrix}, \tag{29}$$

such that $\text{ad}_X Y := [X, Y]$, then (26) yields

$$dK_k(q)(x) = A_k(q) [dH_k(q, x) - a_k(q, x)K_k(q)] \tag{30}$$

$$a_k(q, x) := \begin{pmatrix} 0 & \dots & 0 \\ \sum_{i=1}^v x^{l_i} \text{ad}_{H_{l_i}} & & \vdots \\ 0 & \ddots & \\ \vdots & & \\ 0 & \dots & 0 & \sum_{i=1}^v x^{k_i} \text{ad}_{H_{k_i}} & 0 \end{pmatrix}, \tag{31}$$

$$dH_k(q, x) := \begin{pmatrix} 0 & \dots & 0 \\ \sum_{i=1}^v \partial_{q^{l_i}} H_1 x^{l_i} & & \vdots \\ 0 & \ddots & \\ \vdots & & \\ 0 & \dots & 0 & \sum_{i=1}^v \partial_{q^{k_i}} H_k x^{k_i} & 0 \end{pmatrix}. \tag{32}$$

With canonical coordinates 2. kind, $H_k = \text{diag}(X_1, \dots, X_k)$ is constant, and $dK_k(q)(x) = -A_k(q) a_k(q, x)K_k(q)$. If x is a sufficiently small perturbation,

$$K_k(q + x) = K_k(q) + dK_k(q, x) = (I - A_k a_k)K_k(q). \tag{33}$$

3.5. Kinematics of an MBS with kinematical loops

The kinematic constraints, i.e. the closure conditions on velocity level, are formulated under the condition that $g(q) = 0$. Consider the relative velocity of B_k and B_l , connected by cut-joint $J_a \equiv (l, k)$,

$$\begin{aligned} \text{Ad}_{a,k}^{-1} (V - \text{Ad}_{C_l}^{-1} V) &= \sum_{a \leq N} \text{Ad}_{a,k}^{-1} (K_a - \text{Ad}_{C_l}^{-1} K_a) \dot{q}^a \\ &= \text{Ad}_{e_2}^{-1} \dot{q}^{a_2} \dots \hat{\text{Ad}}_{e_2}^{-1} \dot{q}^{a_v} \text{Z}\dot{q}^{a_1} + \dots + \text{Ad}_{e_2}^{-1} \dot{q}^{a_v} \text{Z}\dot{q}^{a_{v-1}} + \text{Z}\dot{q}^{a_v}. \end{aligned} \tag{34}$$

The last v terms are the twist vectors of the successive screw motions that describe the relative joint motion, expressed in the JFR on B_k . If the motion space of J_a is a SE (3)-subgroup these twists belong to the respective subalgebra.

The kinematic closure condition is the disappearance of the components of the relative velocity, not in this subalgebra. That is, we need to eliminate the twist components in (34) that correspond to the joint motion, which is unconstrained. To formalize this elimination, introduce a selector P^a that restricts the complementary³ $se(3)$ -subspace of the v_a -dimensional space of cut-joint twists, expressed in the JFR on B_k . Application to (34) yields a sufficient set of kinematic constraints for the cut-joint J_a

$$P^a L^a \dot{q} = 0, \tag{35}$$

where $L^a \equiv (L_a^\alpha)$ is the $6 \times N$ matrix with columns

$$L_a^\alpha := \text{Ad}_{a,k}^{-1} (K_a - \text{Ad}_{C_l}^{-1} K_a). \tag{36}$$

This is the standard formulation if the cut-joint's motion space is a subgroup. In this case, the selector also determines the relevant components of the geometric constraints (12). The definition of the joint axes corresponds to the $se(3)$ standard basis, e.g., the e_3 -axis of the JFR is used as joint axis of prismatic/revolute/cylindrical joints and for a planar joint the e_1, e_2 -axes are used as principle axes of translations and e_3 as axis of revolution. Table 2. lists the according selectors for all subgroups.

Combining the constraints (34) for all γ loops yields the system of m kinematic constraints

$$h\dot{q} = 0. \tag{37}$$

The time derivative of (35) yields the dynamic constraints for Λ_a , i.e. the constraints on acceleration level

$$h\ddot{q} + h\dot{q} = 0. \tag{38}$$

The recursions (27), (26) provide a closed form for $\dot{h} = \partial_{q^a} h \dot{q}^a$.

Table 2. Selector P^a for the constrained velocity components of a cut joint J_a of which the motion space corresponds to a subgroup of $SE(3)$

Tablica 2. Selektor P^a za komponentu kinematički ograničene brzine zgloba J_a čiji prostor gibanja odgovara subgrupi $SE(3)$

| DOF / SSG | Motion (Joint type) / Relativno gibanje (vrsta zgloba) | Selector P^a / Selektor P^a |
|-----------|--|---|
| 1 | Translation along fixed axis (prismatic joint) / Translacija duž nepomične osi (translacijski zglob) | $\begin{pmatrix} 1 & 0 & 0 & 0 & 0 & 0 \\ 0 & 1 & 0 & 0 & 0 & 0 \\ 0 & 0 & 1 & 0 & 0 & 0 \\ 0 & 0 & 0 & 1 & 0 & 0 \\ 0 & 0 & 0 & 0 & 1 & 0 \end{pmatrix}$ |
| | Rotation about fixed axis (revolute joint) / Rotacija oko nepomične osi (rotacijski zglob) | $\begin{pmatrix} 1 & 0 & 0 & 0 & 0 & 0 \\ 0 & 1 & 0 & 0 & 0 & 0 \\ 0 & 0 & 0 & 1 & 0 & 0 \\ 0 & 0 & 0 & 0 & 1 & 0 \\ 0 & 0 & 0 & 0 & 0 & 1 \end{pmatrix}$ |
| 2 | Planar translation / Planarna translacija | $\begin{pmatrix} 1 & 0 & 0 & 0 & 0 & 0 \\ 0 & 1 & 0 & 0 & 0 & 0 \\ 0 & 0 & 1 & 0 & 0 & 0 \\ 0 & 0 & 0 & 0 & 0 & 1 \end{pmatrix}$ |
| | Rotation + translation along same axis (cylindrical joint) / Rotacija i translacija oko iste nepomične osi (cilindričan zglob) | $\begin{pmatrix} 1 & 0 & 0 & 0 & 0 & 0 \\ 0 & 1 & 0 & 0 & 0 & 0 \\ 0 & 0 & 0 & 1 & 0 & 0 \\ 0 & 0 & 0 & 0 & 1 & 0 \end{pmatrix}$ |
| 3 | Spatial translation / Prostorna translacija | $\begin{pmatrix} 1 & 0 & 0 & 0 & 0 & 0 \\ 0 & 1 & 0 & 0 & 0 & 0 \\ 0 & 0 & 1 & 0 & 0 & 0 \end{pmatrix}$ |
| | Planar motion (planar joint) / Planarno gibanje (planarni zglob) | $\begin{pmatrix} 0 & 0 & 1 & 0 & 0 & 0 \\ 0 & 0 & 0 & 1 & 0 & 0 \\ 0 & 0 & 0 & 0 & 1 & 0 \end{pmatrix}$ |
| | Spatial rotation (spherical joint) / Prostorna rotacija (sferni zglob) | $\begin{pmatrix} 0 & 0 & 0 & 1 & 0 & 0 \\ 0 & 0 & 0 & 0 & 1 & 0 \\ 0 & 0 & 0 & 0 & 0 & 1 \end{pmatrix}$ |
| 4 | Planar motion + spatial translation (joint macro) / Planarno gibanje + prostorna translacija (složeni zglob) | $\begin{pmatrix} 0 & 0 & 0 & 1 & 0 & 0 \\ 0 & 0 & 0 & 0 & 1 & 0 \end{pmatrix}$ |

³ Notice that this has nothing to do with an orthogonal complement since this would require a metric on $SE(3)$. Furthermore, the particular complement space depends on the specific JFR used to express joint twists.

Remark 5: A problem often encountered, is the dependence of loop constraints, i.e. h permanently a rank less than m . The reason is that for a certain cut-joint a certain number of constraints are formulated, regardless of whether or not the relative motion (to be constrained by the closure condition) can actually take place if the cut-joint is removed. The obvious problem for the formulation of loop constraints, (in particular when automatically generating constraints) is the detection/removal of redundant constraints. Fortunately, one can cope with quite a large class of problems, by noting the geometric background [16].

4. MBS Dynamics

4.1. The Lagrangian motion equations of a MBS with tree structure

Define a frame with origin at the center of mass (COM) of B_k . Let $\overline{M}_k \in SE(3)$ be the transformation from COM-frame of B_k to its RFR. The velocity of the COM-frame is

$$\overline{V}_k = \text{Ad}_{\overline{M}_k}^{-1} V_k \tag{39}$$

With the mass m and the inertia tensor $\Theta_k = (\Theta_{kij})$ of B_k w.r.t. the COM-frame, define the inertia matrix of B_k

$$J_k = \begin{pmatrix} \Theta_k & 0 \\ 0 & m_k I \end{pmatrix} \tag{40}$$

The kinetic coenergy of B_k is then

$$T_k^* = \frac{1}{2} \overline{V}_k^T J_k \overline{V}_k = \frac{1}{2} V_k^T \overline{J}_k V_k, \tag{41}$$

where:

$$\overline{J}_k := \text{Ad}_{\overline{M}_k}^T J_k \text{Ad}_{\overline{M}_k}^{-1}, \tag{42}$$

is the inertia matrix \overline{J}_k of B_k w.r.t. its RFR.

Remark 6: We shall comment on the use of CAD-data here. In section 2.3.3 we abandoned the use of body-fixed RFRs and introduced the formulation (11). We have further seen that the reference configurations are $m = I$ since CAD-systems relate to all quantities to a world frame, which in the reference frame coincides with the RFR. An analogous argument holds for the inertia data, so that CAD-system already determine J . In summary, local RFRs are completely dispensable.

The total kinetic coenergy of the MBS is $T^* := \sum_k T_k^*$. In terms of generalized velocities, this is the quadratic

form $T^*(q, \dot{q}) = \frac{1}{2} g_{ab}(q) \dot{q}^a \dot{q}^b$, with the symmetric

$$g_{ab} := \sum_{k=b}^N K_{k^a}^T K_{k^b}, a \leq b. \tag{43}$$

Besides singularities of our parameterization of the configuration space, g_{ab} is positive definite. Hence g_{ab} defines a metric on the tangent space $T_q \mathbb{V}^n$ in every point q , which makes \mathbb{V}^n a Riemannian space.

In the Lagrangian framework, the dynamics of a holonomic MBS are governed by the Lagrangian motion equations (LME) of second kind

$$\frac{d}{dt} (\partial_{\dot{q}^a} \Lambda) - \partial_{q^a} \Lambda = Q_a^0, \tag{44}$$

where the Lagrangian $\Lambda(q, \dot{q}) := T^*(q, \dot{q}) - U(q)$ is given in terms of the kinetic coenergy and the potential energy U . Q_a^0 are generalized forces not covered by the Lagrangian, such as dissipation or control forces.

The LME for a skleronomic holonomic MBS with tree topology are [13]:

$$g_{ab}(q) \ddot{q}^b + \Gamma_{abc}(q) \dot{q}^b \dot{q}^c = Q_a, \tag{45}$$

with $Q_a := Q_a^0 - \partial_{q^a} U$ and the Christoffel symbols of the first kind:

$$\Gamma_{abc} = \frac{1}{2} (\partial_{q^b} g_{ac} + \partial_{q^c} g_{ab} - \partial_{q^a} g_{bc}) = \Gamma_{acb}. \tag{46}$$

In view of (27) they can be expressed as:

$$\Gamma_{abc} = \frac{1}{2} \sum_{k=c}^n (K_{k^c}^T \overline{J} ad_{k^a} K_{k^b} + K_{k^b}^T \overline{J} ad_{k^a} K_{k^c} + K_{k^a}^T \overline{J} ad_{k^c} K_{k^b}) a < b \leq c \text{ or } b \leq a < c, r = \max(a, b), s = \min(a, b). \tag{47}$$

Relation (47) can be simplified using Binet's inertia tensor:

$$\Gamma_{abc} = \sum_{k=c}^n K_{k^b}^T \tilde{J} ad_{\Omega(K_k^c)} K_{k^a}, a < b \leq c \text{ or } b \leq a < c, \tag{48}$$

where $\tilde{J} := Ad_{M^{-1}}^T \text{diag}(\vartheta, m_k I) Ad_{M^{-1}}$ and $\Omega(X) = \omega$ gives the angular part of the twist $X = (\omega, v)$.

In matrix notation, the LME are expressed as:

$$G(q) \ddot{q} + C(q, \dot{q}) \dot{q} = Q, \tag{49}$$

where

$$G(q) := (g_{ab}), C(q, \dot{q}) := (\Gamma_{abc} \dot{q}^c), Q := (Q_a), \tag{50}$$

G is the generalized mass matrix, $C\dot{q}$ represents generalize Coriolis and centrifugal forces, and Q covers all potential forces and remaining forces not represented by the Lagrangian Λ . With (24), and (30) follows:

$$G(q) = K^T JK \in \mathbb{R}^{n,n} \tag{51}$$

$$C(q, \dot{q}) = K^T (b^T J - J A a) K, \tag{52}$$

where $\bar{J} := \text{diag}(\bar{J}_1, \dots, \bar{J}_k)$, and b only depending on the body twists $V = K_k \dot{q}_k$:

$$b(V) := \text{diag}(ad_{V_1}, \dots, ad_{V_N}) \in \mathbb{R}^{6N,6N} \tag{53}$$

The first term in the brackets of (52) represents gyroscopic forces, due to the fact that $\dot{q}^T K^T b^T JK \dot{q} = V^T b^T J V \equiv 0$, since $b(V) V \equiv 0$. Hence, one can separate a gyroscopic potential from the Lagrangian Λ , which contributes to gyroscopic forces.

4.2. The Lagrangian motion equations of a constrained MBS

Using relative coordinates, an MBS with kinematic loops is a tree-topology system subject to a system of r holonomic constraints (13). More generally, an MBS is subject to further geometric and/or non-holonomic velocity constraints. Denote the overall system of m geometric constraints by $f^k(q) = 0$, and with $f_a^{a_1}(q) \dot{q}^a = 0$ the overall system of $r = |\{a_1\}| \geq m$ (linear) velocity constraints. The geometric constraints define the configuration space of the constrained MBS $V := \{q \in \mathbb{V}^n | f^k(q) = 0\}$. For simplicity we presume $\text{rank}(\partial_{q^a} f^k) = m$ and $\text{rank}(f_a^{a_1}) = r$ on all V . Then V is a $n - m$ -dimensional smooth manifold.

There exists a partitioning $(f^{b_1 a_1}) = f^{b_1 a_1} | f^{b_2 a_2}$ with $\text{rank}(f^{b_1 a_1}) = r$, and thus an orthogonal complement $F_{a_2}^{a_1}$ of $f_a^{a_1}$ with $\text{rank}(F_{a_2}^{a_1}) = n - r$, i.e. $f^{a_1 a_1} F_{a_2}^{a_1} = 0$. Hence, the system of kinematic constraints has a solution:

$$\dot{q}^a = F_{a_2}^{a_1}(q) \dot{q}^{a_2}, \quad q \in V. \tag{54}$$

(54) is a parametrization of the $n - r$ -dimensional vector space defined by the velocity constraints - a subspace of the $n - m$ -dimensional tangential space $T_q V$. I.e. the vector space of admissible velocities may have a lower dimension than the base manifold V . We use primed indices to indicate reference to this subspace. The solution (54) is not unique and a different choice of the partitioning yields a different chart.

The motion equations for the constrained MBS in terms of \dot{q}^{a_2} follow by substitution of \dot{q}^a , using (54), [13]:

$$g_{a_2 b_2} \dot{q}^{b_2} + \Lambda_{a_2 b_2 c_2} \dot{q}^{b_2} \dot{q}^{c_2} = Q_{a_2}, \tag{55}$$

$$\text{with the metric } g_{a_2 b_2} := g_{ab} F_{a_2}^{a_1} F_{b_2}^{a_1}, \tag{56}$$

the generalized Christoffel symbols of first kind:

$$\Lambda_{a_2 b_2 c_2} := (\Gamma_{abc} - g_{ac} \tilde{f}^{c_1 a_1} \partial_{q^{c_1}} f^{a_1 b_1}) F_{a_2}^{a_1} F_{b_2}^{a_1} F_{c_2}^{a_1}, \tag{57}$$

where $(\tilde{f}^{c_1 a_1}) := (\tilde{f}^{a_1 c_1})^{-1}$, and the generalized forces $Q_{a_2} := F_{a_2}^{a_1} Q_{a_1}$. The equations (55) are the equations of Woronetz. Assuming regularity of F_a , (56) defines a metric on V .

The Woronetz equations can be written in matrix form:

$$\bar{G}(q) \dot{q}_2 + \bar{C}(q, \dot{q}) \dot{q}_2 + \bar{N}(q) = \bar{Q}, \tag{58}$$

where

$$\bar{G} := F^T G F, \quad \bar{C} := F^T (C F + G \dot{F}), \quad \bar{N} := F^T N, \quad \bar{Q} := F^T Q. \tag{59}$$

The system (55) together with the kinematic constraints $f^{a_1 a_1}(q) \dot{q}^{a_1} = 0$ yield n differential equations in $q \in \mathbb{V}^n$, which completely describe the MBS dynamics.

The constraints are holonomic if and only if the integrability conditions $A^{b_1} \equiv 0$ are satisfied, where:

$$A_{b_2 c_2}^{b_1 c_1} := F_{b_2}^{b_1} F_{c_2}^{c_1} (\partial_{q^{c_1}} f^{c_1} - \partial_{q^{c_1}} f^{c_1}) \tag{60}$$

is called the object of non-holonomy.

5. Numerical integration of MBS Dynamics

5.1. ODE integration

As explained, the LME (45) yield an ODE system on the state space $T \mathbb{V}^n$, where n ODE is assumed. $T \mathbb{V}^n$ is a tangential bundle that comprises configuration manifold \mathbb{V}^n and union of all tangential spaces $T_q \mathbb{V}^n$. It is a $2n$ -dimensional manifold covered by the coordinates $q, \dot{q}: T \mathbb{V} = \{(q, \dot{q}) : q \in \mathbb{V}, \dot{q} \in T_q \mathbb{V}\}$. By adopting the generalized mass matrix $G(q)$ as a Riemannian metric on the configuration manifold, the tangential space $T_q \mathbb{V}$ ("the fiber of the tangential bundle at point q ") becomes a locally Euclidean vector space spanned by a covariant basis \hat{g}_{q_i} . The LME can be written in the shorter matrix form as:

$$G(q) \ddot{q} = Q^*(q, \dot{q}, t), \tag{61}$$

and following the standard procedure, it can be turned into the $2n$ ODE form:

$$\begin{aligned} \dot{v} &= G^{-1}(q) Q^*(q, v, t), \quad \dot{q} = v, \quad \bar{q} = \begin{bmatrix} q \\ v \end{bmatrix}. \\ \dot{x} &= f(\bar{x}), \quad f(\bar{x}) = \begin{bmatrix} v \\ G^{-1} Q^* \end{bmatrix}. \end{aligned} \tag{62}$$

The solution of (62) is the integral curve of the vector field $f(\bar{x})$ on tangential bundle ("velocity phase space") for a set of Cauchy data (t_0, \bar{x}_0) .

5.2. DAE integration

If additional holonomic/nonholonomic constraints are imposed on the system, instead of reducing the system to the constrained LME form as explained in chapter 4.2,

one can model the system using a mathematical model in descriptor form. This is straightforward modelling procedure that can be easily applied for a wide class of MBS (thus being a basis for many general MBD packages), but it leads to DAE integration (numerical integration of system of differential-algebraic equations) that is generally more formidable differential-algebraic than standard ODE integration routine.

To avoid high-index DAE formulations, the mathematical model for dynamic simulation of multibody systems with imposed holonomic constraints $\Phi(q, t) = 0$ and $\Phi_q^*(q, t) \dot{x} = 0$, where $\Phi(q, t) := (f^k(q, t))$ and $\Phi_q^* := (\partial_{q_i} f^k)$, is often shaped as a differential-algebraic system (DAE) of index 1 (redundant coordinates formulation, ideal constraints' reaction forces are assumed)

$$\begin{bmatrix} G & \Phi_q^{*T} \\ \Phi_q^* & 0 \end{bmatrix} \begin{bmatrix} \ddot{q} \\ \lambda \end{bmatrix} = \begin{bmatrix} Q^* \\ \zeta \end{bmatrix}, \tag{63}$$

where the Lagrangian equations of the first type:

$$G(q) \ddot{q} + \Phi^{*T}(q, t) \lambda = Q^*(q, q, t) \tag{64}$$

$$q \in \mathbb{R}^n, \Phi_q^{*T} \in \mathbb{R}^{m \times n}, \text{rank}[\Phi_q^*] = m,$$

and the constraint equations at the acceleration level

$$\Phi_q^*(q, t) \ddot{q} = \zeta, \tag{65}$$

are put together. System (63) is uniquely solvable for the set of consistent initial values. It can be integrated in time to obtain the motion of the system as well as the constraint reactions. Although constraints at the acceleration level will be immanently satisfied, since (65) is included in mathematical model (63) and will be explicitly solved during integration, the numerical non-stability of (65) can induce constraints violation at both the position and velocity level.

As explained, holonomic constraints restrict system configuration space and impose constraints at velocity level: a trajectory $T: q^i = q^i(t)$ is "forced to move" on the $n - m$ dimensional constraint manifold $\mathbb{V}^{n-m}(t) = \{q \in \mathbb{V}^{n-m}, \Phi(q, t) = 0\}, t \geq 0, q(t_0) \in \mathbb{V}^{n-m}(t_0)$ and linear constraint equation (66) is imposed at system velocities:

$$\Phi_q^*(q, t) \dot{x} = -\Phi_t. \tag{66}$$

Although analytical solution curves for consistent initial conditions will move on a tangential bundle $T^{n-m} \mathbb{V}^{n-m}$ (having satisfied all constraints imposed on the system), a numerical solution will tend to drift away from constraint manifold.

If, beside holonomic constrains, additional non-holonomic constraints given in linear (Pfaffian) form are imposed on the system (further reducing dimensionality of admissible velocities by forming subspace at $T_q \mathbb{V}$), a mathematical model similar to (63) can be introduced [38], allowing the same integration procedure as for the holonomic systems.

5.3. Stabilization of constraint violation

If the governing equations of the system are based on a mathematical model in descriptor form, leading to time integration of redundant coordinates, a constraint violation stabilization method has to be applied during the integration procedure. Alternatively, a well-known algorithm described in [39] can be used. It is based on a coordinate partitioning procedure prior to integration, followed by the time integration of the selected independent coordinates only. Another projective stabilization procedure is described in [3].

The stabilization algorithm proposed in [38] is based on projection of the steppost-integration results (system current state point) to the constraint manifold in the course of simulation. An advantage of the procedure is straightforward integration of dynamic equations, while stabilization algorithm is to be applied only after intolerable constraint violation is detected. The procedure can be briefly described as follows.

If constraint violation (specified by given numerical tolerances) occurs after step-integration phase, the "position" stabilization step is to be performed by correcting dependent coordinates sub-vector q^{dep} via solving system constraint equation, providing thus shifting of the system configuration-point q back to constraint manifold \mathbb{V}^{n-m} . The procedure is then repeated at the velocity level by correcting \dot{q}^{dep} to bring \dot{q} in accordance with (66). This means that, as stabilization step final result, time-integration values q, \dot{q} are projected to the constraint manifold tangential bundle $T \mathbb{V}$, thus completely satisfying constraints of the system. As will be seen later, a crucial point of the algorithm is appropriate selection of sub-vectors q^{dep} and \dot{q}^{dep} to provide the optimal stabilization effect.

Criteria for coordinates selection can be expressed geometrically: basically, every selection that returns sub-vector of dependent coordinates q^{dep} whose basis vectors have non-zero projections on the constraint subspace \mathbb{C}_q^m (corresponding $m \times m$ sub-matrix of constraint matrix Φ_q^* is non-singular) is a correct one and can be used for stabilization procedure. Consequently, basis vectors of independent coordinates q^{ind} must have projections on tangential space of constraint manifold $T_q \mathbb{V}^{n-m}$ that complement \mathbb{C}_q^m . If the extracted sub-vectors do not satisfy specified conditions, selection is not a valid one and calculation will fail.

5.3.1. Numerical errors along configuration manifold

The main problem that may occur during stabilization procedure is an inadequate coordinate selection that may have a negative effect on integration accuracy along the constraint manifold. Although, as was explained, every

partitioning that returns acceptable sub-vectors can be used for stabilization, a non-optimal choice of coordinate sub-vectors may cause an increase of numerical errors along the manifold during stabilization part of the integration procedure. If this happens, a correction of constraint violation will be accomplished at the expense of “kinetic motion” accuracy that comes as a result of ODE integrators of system variables \dot{q}, q .

The “mechanism” of emerging of numerical errors along configuration manifold, because of an inadequate partitioning during the stabilization procedure is outlined in Figure 3. For illustrative simplicity, holonomic (as well as scleronomic) example $q = x \in \mathbb{V} \equiv \mathcal{M}^2$, rank $[\Phi_x^*] = 1$, $\mathbb{V}^{n-m} = \mathbb{S}^1$ is discussed. Fundamentally, nothing is changed if more general case is analysed.

Assuming that, starting from ①, an integration of ODE gives result ③ instead of exact position ②, a projection on the constraint manifold \mathbb{S}^1 by adjusting coordinate x^1 (solving constraint equation along x^1 curve) yields result ④ which is consistent to the constraint. If instead of x^1 , the variable x^2 was chosen to be a dependent coordinate, an adjustment of the integration result along x^2 curve would yield solution ⑤, which is also consistent with the constraint but contains considerable error along the manifold \mathbb{S}^1 . A remedy for the problem of an inadequate selection of dependent coordinates has been described in [2], where a projective criterion to the coordinate partitioning method is discussed.

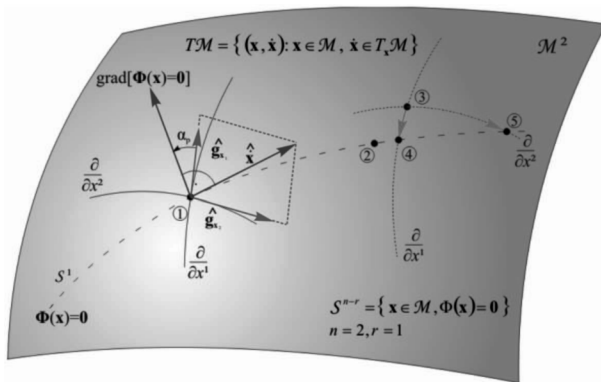


Figure 3. Numerical correction of the constraint violation at the configuration (“generalized position”) level

Slika 3. Numerička korekcija povreda kinematičkih ograničenja na nivou poopćenih položaja

5.3.2. Criterion for optimized coordinates partitioning

In the framework of constraint violation stabilization algorithm proposed in [38], the main idea of “controlling” the numerical error that is eventually introduced during stabilization projection step is to “minimize” the artificial numerical shift along the manifold by projecting integration point “as direct as possible using

coordinate curves” to the constraint manifold. This can be accomplished by utilizing criterion for optimized partitioning that allows for determination of those coordinates whose direction vectors \hat{g}_{q_i} are directed most orthogonally toward constraint manifold. By selecting these coordinates as dependent ones during projection procedure, the constraint equation would be solved along the selected “orthogonally directed” curves $\frac{\partial}{\partial q_i}$, providing thus optimized projection and “controlled” numerical error along the manifold. The basic idea of the criterion is to determine those m coordinates whose direction vectors \hat{g}_{q_i} deliver the biggest relative projections to the \mathbb{C}_q^m (i.e. “small” value of α_p , Figure 3) and select them as dependent variables which will be adjusted during the stabilization procedure. By correcting coordinates whose direction vectors align well with the constraint gradients, it is ensured that correction procedure will shift a state-point of the system “as direct as possible using coordinate curves” to constraint “hyper-surfaces”, minimizing thus an error along constraint manifold. Alternatively, the coordinates that have “good” projections on the local tangential space $T_q \mathbb{V}^{h-m}$ can be extracted and treated as independent coordinates [37].

The main “measure” for expressing the criterion is relative length of the projection of the coordinates direction vectors \hat{g}_{q_i} to the constraint subspace \mathbb{C}_q^m (or tangent subspace $T_q \mathbb{C}^{n-m}$). The relative lengths of constraint subspace projection and tangent subspace projection are given by (67) and (68):

$$\Delta_C = \frac{\|\hat{g}_{q_i}\|_{CTC}^2}{\|\hat{g}_{q_i}\|_G^2}, \tag{67}$$

$$\Delta_T = \frac{\|\hat{g}_{q_i}\|_{CTT}^2}{\|\hat{g}_{q_i}\|_G^2}, \tag{68}$$

where the squared length of the projections and $\|\hat{g}_{q_i}\|_{CTT}^2$ (length of the projections of \hat{g}_{q_i} on the subspace \mathbb{C}_q^m and subspace $T_q \mathbb{V}^{n-m}$ respectively) and $\|\hat{g}_{q_i}\|_G^2$ is the squared length of \hat{g}_{q_i} in the natural basis \mathbf{G} . Those coordinates which have the biggest Δ_C should be chosen as dependent coordinates and those with the biggest Δ_T are pertinent for independent variables. Of course, squared length indicated in denominator of the equations (67) and (68) should be calculated with respect to the system manifold Riemannian metric G , while expressions in nominator must be calculated via sub-metrics associated with the constraint subspace and its orthogonal counterpart, as explained in [2, 39]).

5.4. Numerical example

5.4.1. Mechanical system with non-holonomic constraint

In the framework of the first numerical example that presents numerical forward dynamics of the satellite motion while its panel system develops, the effect of

the described constraint stabilization procedure will be illustrated without details on mathematical modeling of the satellite dynamics (for more details, refer to [38]).

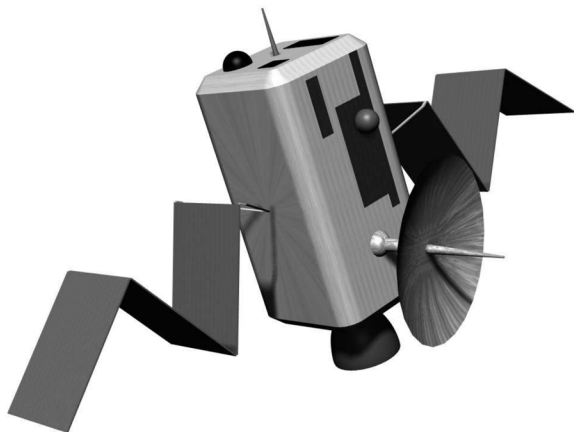


Figure 4. Satellite multibody model
Slika 4. Mehanički model satelita

The considered satellite is based on the INTELSAT V satellite [35]; it consists of a main body and two panels of four parts (Figure 4). A planar model is used, and no gravitational force is incorporated in the simulation. Since angular momentum of the system is conserved, the additional constraint equation that express conservation of the angular momentum is imposed on the system during part of the analysis (it can be treated as non-holonomic constraint as it involves kinematic constraint at the velocity level which cannot be directly transposed to the generalized positions level).

The equations of motion of the satellite were obtained symbolically starting from (45) using Mathematica programming package. Forward dynamics of the satellite was performed for a duration time of 10 s with a variable step Runge-Kutta method of mixed order (4th and 5th) using an absolute tolerance of $1e-18$. The purpose of this simulation is to obtain a reference trajectory which can be treated as the “exact” solution. The maximum error on the total energy, which should be constant, is $1,1e-9$ J and the maximum error on the total angular momentum is $1,6e-9$ kg·m²/s. Note that no constraint stabilization was performed in the process of obtaining reference trajectory. After obtaining reference solution, dynamic simulation was performed using a Euler first order numerical integration scheme and a fixed timestep of 0,01 s. As Figure 5 shows, the total angular momentum of the satellite (about the center of mass) is not constant, and the error grows steadily. These errors were eliminated during subsequent stabilized integration that utilized described projection algorithm by considering system constraint manifold defined via additional nonholonomic constraint equation of angular momentum conservation (Figure 5).

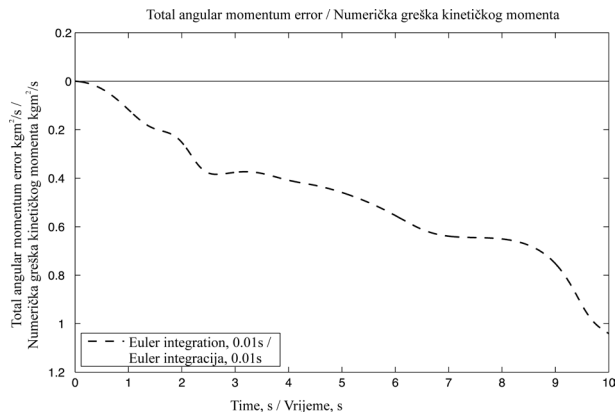


Figure 5. Total angular momentum error versus time

Slika 5. Numerička greška kinetičkog momenta oko središta masa sustava

5.4.2. Mechanical system with mixed holonomic and non-holonomic constraints

The second numerical example focuses on the numerical forward dynamics of a snakeboard. The mathematical model of the snakeboard is synthesized using descriptor formulation, resulting in a mix of holonomic and nonholonomic constraints. To investigate characteristics of optimized generalized coordinates partitioning procedure when holonomic and non-holonomic constraints are present in the system, the separate partitioning at position level and velocity level is performed and analyzed. It is shown that optimal selection of independent coordinates is not necessarily the same as the best set of independent velocities.

The snakeboard is illustrated in Figure 6. It is modelled as a planar multibody system with 4 bodies connected to each other by means of pin-joints. There is one coupler (B), two small boards with wheels (A and C) and one rotor (D) on the coupler to model dynamical excitation of human body torso motion. The two pairs of wheels cannot slide and therefore impose two non-holonomic constraints on the system. At the configuration level, the snakeboard has 6 DOF.

The snakeboard is mathematically modelled in descriptor form, i.e. at the configuration level each component has 3 degrees of freedom and holonomic constraints are added to model the joints. Therefore, the mathematical model is synthesised using 12 coordinates and 6 holonomic constraints, supplemented by additional 2 non-holonomic constraints.

The chosen coordinates are (x_i, y_i, θ_i) representing the position of the center of mass and the global orientation of body $i = A, B, C$ or D .

During performing forward dynamic analysis, the following scenario was considered. The snakeboard is actuated by a force with constant amplitude acting on

the system centre of mass and with varying orientations parallel to the coupler, towards the front wheels. The wheels are forced into a sinusoidal motion of 1 Hz and amplitude of 0,5 rad by means of PD-controllers ($P = 10 \text{ N/m}$, $D = 0,1 \text{ N}\cdot\text{s/m}$). The forward dynamics was first performed using Runge-Kutta method of mixed order (4th and 5th) using an absolute tolerance of $1e-18$ to obtain a reference simulation presented in Figure 7.

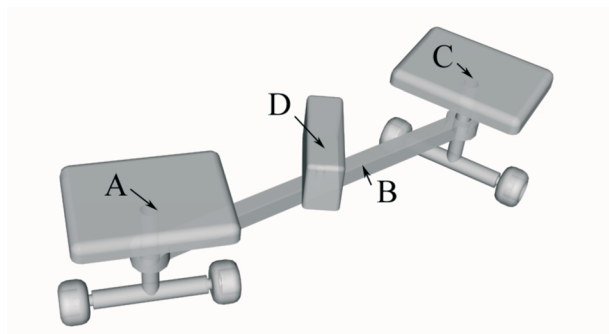


Figure 6. Snakeboard multibody model
Slika 6. Mehanički model 'snakeboard-a'

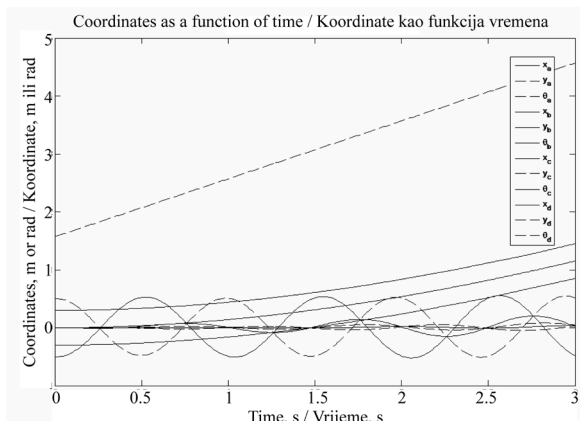


Figure 7. System reference generalized coordinates
Slika 7. Referentne poopćene koordinate položaja sustava

For the analyzed motion, the relative projections of the configuration coordinates and velocity coordinates on the respective constraint manifolds were calculated and presented in Figure 8. (configuration coordinates projections are presented left and velocities are right).

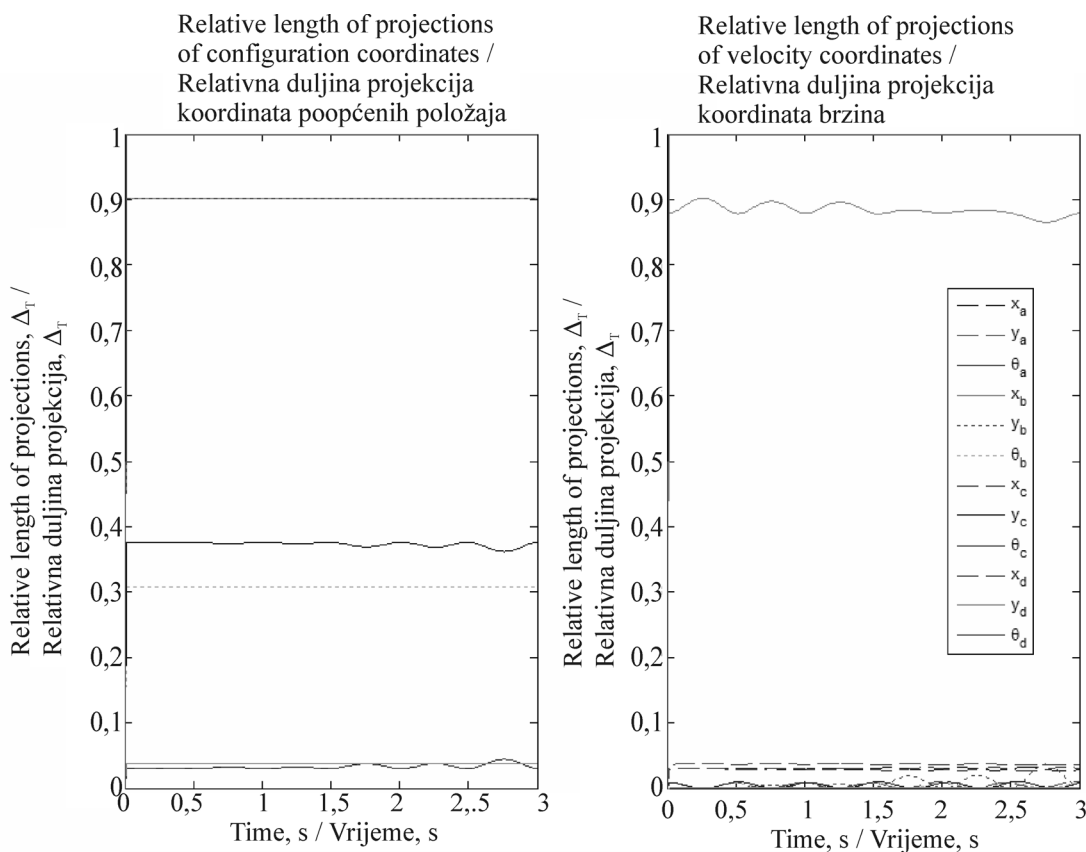


Figure 8. Relative length of projection for configuration coordinates and velocity coordinates
Slika 8. Relativna duljina projekcija baznih vektora na višestrukost ograničenja

As one can see, there are clear differences between the lengths of relative projections at both levels. Since the coordinate which has smaller projection at the respective constraint manifold would be a more appropriate choice for dependent integration parameter than one with longer projection, it is clear that optimal choices for dependent position coordinates would differ from those for velocities.

In the sequel, the performance of constraint violation stabilization procedure based on optimal coordinates partitioning, is discussed in the framework of the presented example. For this purpose, only constraint stabilization at velocity level is considered. In order to determine and compare local integration/stabilization velocity errors, the integration procedure was performed as follows. The state vector of the reference trajectory has been integrated using fixed step Euler numerical integrator at any given time for one single step (0.01 s) with and without projective stabilization step and the difference between the stabilized and unstable solution has been calculated. This procedure was followed twice, with a different choice of dependent coordinates in the case of stabilized solution: once with optimal stabilization (as shown in Figure 8) and once with a suboptimal set of dependent coordinates (the coordinate with smallest projection is replaced with the 7th smallest one).

The errors ε were calculated by integrating the weighted squared difference (using system metric \mathbf{M}) in velocity between both sets of trajectories:

$$\varepsilon = \int_{t=0}^{t_{\text{end}}} (\Delta \dot{q}^T \mathbf{M} \Delta \dot{q}) dt.$$

The obtained result shows that error between the unstabilized fixed step solution and the optimal solution is $0,00003e-5$, while the difference between unstabilized and the suboptimal solution is significantly larger and yields $0,47836e-5$. The comparison between the errors shows that during integration step, the distance from solution before (i.e. after unstable ODE step that violates constraints) and after constraint stabilization is smaller when dependent coordinate is chosen according to projective criterion. As one could have expected, this means that the additional stabilization step, based on optimized partitioning, shifts unstable ODE numerical solution back to the constraint manifold with controlled error along the manifold (see [38] for details). However, as has been shown previously, for non-holonomic systems the optimized coordinates partitioning should be done separately at position and velocity level.

Acknowledgments

The authors acknowledge dr. Joris Naudet (University of Brussels, VUB) for performing computations in the framework of presented numerical example.

REFERENCES

- [1] ANDERSON, K.: *An Order n Formulation for the Motion Simulation of General Multi-Rigid-Body Constrained Systems*, Computers & Structures, 43, (1992) 3, 565-579.
- [2] BLAJER, W.; SCHIEHLEN, W. and SCHIRM, W.: *A Projective Criterion to the Coordinate Partitioning Method for Multibody Dynamics*, Archive of Applied Mechanics, 64, (1994), 86-98.
- [3] BLAJER, W.: *Elimination of Constraint Violation and Accuracy Aspects in Numerical Simulation of Multibody Systems*, Multibody System Dynamics, 7, (2002), 265-284.
- [4] BROCKETT, R. W.; STOKES, A.; PARK, F. C.: *Geometrical Formulation of the Dynamical Equations Describing Kinematic Chains*, IEEE Int. Conf. on Robotics and Automation, (1993), 637-642.
- [5] BULLO, F.; LEWIS, A. D.: *Geometric Control of Mechanical Systems*, Springer, 2005.
- [6] DAI, J. S.: *An historical review of the theoretical development of rigid body displacements from Rodrigues parameters to the finite twist*, Mech. Mach. Theory, 41, (2006), 41-52.
- [7] FEATHERSTONE, R.: *The Calculation of Robot Dynamics Using Articulates-Body Inertias*, Int. J. Robotics Research, 2, (1983) 1, 13 - 30.
- [8] FIJANY, A.; SHARF, I.; D'ELEUTERIO, G.: *Parallel $O(\log N)$ Algorithms for Computation of Manipulator Forward Dynamics*, IEEE Trans. Rob. and Automation, 11, (1995) 3, 389-399.
- [9] FUNDA, J.; TAYLOR, R. H.; PAUL, R. P.: *On homogenous transformations, Quaternions, and Computational efficiency*, IEEE Trans. on Robotics and Automation, 6, June (1990) 3, 382-388.
- [10] HAIRER, E.; Lubich, C.; Wanner G.: *Geometric Numerical Integration*, Springer, 2002.
- [11] HERVE, J. M.: *Intrinsic formulation of problems of geometry and kinematics of mechanisms*. Mech. Mach. Theory, 17, (1982) 3, 179-184.
- [12] LEWIS, D.; SIMO, J. C.: *Conserving Algorithms for the Dynamics of Hamiltonian Systems on Lie Groups*, J. Nonlinear Sci., 4, (2004), 253-299.
- [13] MAISSER, P.: *A Differential Geometric Approach to the Multibody System Dynamics*, ZAMM, Z. angew. Math. Mech., 71, (1991) 4, 116-119.
- [14] MCCARTHY, J. M.: *Geometric Design of Linkages*, Springer-Verlag, New York, 2000.
- [15] MORAWIEC, A.: *Orientations and Rotations*, Springer, 2004.
- [16] MÜLLER, A.: *A Conservative Elimination Procedure for Redundant Closure Constraints in MBS Models*, Multibody Systems Dynamics, Springer, 16, (2006) 4, 309-330.
- [17] MÜLLER, A.; Maisser, P.: *Lie group formulation of kinematics and dynamics of constrained MBS and its application to analytical mechanics*, Multibody System Dynamics, 9, (2003), 311-352.

- [18] MÜLLER, A.: *Geometric characterization of the configuration space of rigid body mechanisms in regular and singular points*, 29th Mechanisms & Robotics Conference, ASME 2005 International Design Engineering Technical Conferences, September 22-28, 2005, Long Beach, California, USA.
- [19] MÜLLER, A.: *On Non-Smooth Phenomena in the Kinematics of Rigid Body Mechanisms*, Multibody Dynamics 2007, ECCOMAS Thematic Conference, 25-28 June 2007, Milano, Italy.
- [20] MURRAY, R. M.; LI, Z.; SASTRY, S. S.: *A mathematical Introduction to robotic Manipulation*, CRC Press, 1993.
- [21] MURRAY, R. M.; SASTRY, S. S.: *Nonholonomic motion planing: steering using sinusoids*, IEEE Trans. Autom. Control, 38, (1993) 5, 700-716.
- [22] ORTEGA, R. et al: *Passivity-based Control of Euler-Lagrange-Systems*, Springer, 1998.
- [23] OSTROWSKI, J.: *Geometric Perspectives on the Mechanics and Control of Robotic Locomotion*, 7th Int. Symp. Robotics Research, Munich, Germany, Oct. 1995; in G.Giralt, G. Hitzinger (Eds), Robotics Research, Springer-Verlag, 1996.
- [24] PARK, F. C.; BOBROW, J. E.; PLOEN, S. R.: *A Lie Group Formulation of Robot Dynamics*, Int. J. Robotics Reserch, 14, (1995) 6, 609-618.
- [25] PARK, F. C.: *Distance metrics on the rigid-body motions with applications to mechanism design*, ASME Journal of Mechanical Design, 117, (1995) 1, 48-54.
- [26] PARK, F. C.; CHOI, J.; PLOEN, S. R.: *Symbolic formulation of closed chain dynamics in independent coordinates*, Mech. Mach. Theory, 34, (1999), 731-751.
- [27] PARK, J.; CHUNG, W.-K.: *Geometric Integration on Euclidean Group With Application to Articulated Multibody Systems*, IEEE Trans. Robotics, Vol. 21, No. 5, 2005, pp. 850-863.
- [28] PLOEN, S. R.; PARK, F. C.: *Coordinate-Invariant Algorithms for Robot Dynamics*, IEEE Trans. Robotics and Automation, 15, (1999) 6, 1130-1135.
- [29] PAPASTAVRIDIS, J. G.: *Analytical Mechanics*, Oxford University Press, 2002.
- [30] RICO, J. M.; GALLARGO, J.; RAVANI, B.: *Lie Algebra and the Mobility of Kinematic Chains*, Journal of Robotics System, 20, (2003) 8, 477-499.
- [31] RICO, J. M.; RAVANI, B.: *On mobility analysis of linkages using group theory*, ASME Journal of Mechanical Design, 125, March (2003), 70-80.
- [32] RODRIGUEZ, G.; KREUTZ-DELGADO, K.: *Spatial operator factorization and inversion of the manipulator mass matrix*, IEEE Trans. Robotics and Automation, 8, (1992) 1, 65 - 76.
- [33] SAHA, S. K.; SCHIEHLEN, W. O.: *Recursive Kinematics and Dynamics for Parallel Structured Closed-Loop Multibody Systems*, Mech. Struct. & Mach., 29, (2001) 2, 143-175.
- [34] SELIG, J. M.: *Geometrical methods in robotics*, Springer, 1996.
- [35] WIE, B.: *Space Vehicle Dynamics and Control*, AIAA, 1998.
- [36] WOLF, A.; SHOHAM, M.: *Screw theory tools for the synthesis of the geometry of a parallel robot for a given instantaneous task*, Mech. Mach. Theory, 41, (2006), 656-670.
- [37] TERZE, Z.; LEFEBER, D.: *Dynamic Simulation of Multibody Systems With no Constraints Violation*, Transactions of FAMENA, 24, (2000), 1-9.
- [38] TERZE, Z.; NAUDET, J.: *Geometric Properties of Projective Constraint Violation Stabilization Method for Generally Constrained Multibody Systems on Manifolds*, Multibody System Dynamics, 20, (2008), 85-106.
- [39] TERZE Z. et al: *Null Space Integration Method for Constrained Multibody System Simulation with no Constraint Violation*, Multibody System Dynamics, 6, (2001), 229-243.
- [40] WEHAGE, R. A. and HAUG, E. J.: *Generalized Coordinate Partitioning for Dimension Reduction in Analysis of Constrained Dynamic Systems*, Journal of Mechanical Design, 104, (1982), 247-255.
- [41] ZEFRAN, M.; KUMAR, V.; CROKE, C.: *Choice of Riemannian Metric for Rigid Body Kinematics*, Proc. ASME 1996 Inte. Design Engineering Technical Conferences, August 19-22, 1996, Irvine, California, USA 29.